

# Influence of cell fate mechanisms upon retinal mosaic formation: a modelling study

Stephen J. Eglen<sup>\*,†</sup> and David J. Willshaw

Institute for Adaptive and Neural Computation, School of Informatics, University of Edinburgh, Edinburgh EH1 2QL, UK

<sup>\*</sup>Present address: Department of Anatomy and Neurobiology, Washington University School of Medicine, 660 S. Euclid, St Louis, MO 63110, USA

<sup>†</sup>Author for correspondence (e-mail: eglen@pog.wustl.edu)

Accepted 29 August 2002

## SUMMARY

Many types of retinal neurone are arranged in a spatially regular manner so that the visual scene is uniformly sampled. Several mechanisms are thought to be involved in the development of regular cellular positioning. One early-acting mechanism is the lateral inhibition of neighbouring cells from acquiring the same fate, mediated by Delta-Notch signalling. We have used computer modelling to test whether lateral inhibition might transform an initial population of undifferentiated cells into more regular populations of two types of differentiated cells. Initial undifferentiated cells were positioned randomly, subject only to a minimal distance constraint. Each undifferentiated cell then acquired either primary or secondary fate using one of several lateral inhibition mechanisms. Mosaic regularity was assessed using the regularity index and the packing factor. We found that for irregular undifferentiated mosaics, the arrangement of resulting primary (but not secondary) fate cells was more regular than in the initial undifferentiated population.

However, for regular undifferentiated mosaics, no further increases in the regularity of the primary fate mosaics were observed. We have used this model to test the specific hypothesis that on- and off-centre retinal ganglion cells emerge from an initial, irregular undifferentiated population of ganglion cells. Lateral inhibition can subdivide an initially irregular population into two types of cell that are mildly regular. However, lateral inhibition alone is insufficient to produce mosaics of the same regularity as observed experimentally. Likewise, and in contrast to earlier reports, cell death alone is insufficient to match the regularity of experimental mosaics. We conclude that lateral inhibition can transform irregular distributions into regular mosaics, upon which subsequent processes (such as lateral cell movement or cell death) can further refine mosaic regularity.

Key words: Retinal mosaics, Cell fate, Cell death

## INTRODUCTION

Many types of retinal cells are distributed regularly across the retina (Cook and Chalupa, 2000). This regular arrangement is assumed to help uniform spatial processing of the visual world. Several developmental mechanisms are thought to be involved in arranging cells into a regular distribution, including spatial control of cell fate (Frankfort and Mardon, 2002), lateral migration (Reese et al., 1995) and cell death (Jeyarasasingam et al., 1998). For a recent review of the experimental literature, see Cook and Chalupa (Cook and Chalupa, 2000). Each of these mechanisms could act at different times during development to transform an initially irregular array of cells into a more regular distribution as seen in adulthood. In this paper, we address the potential role that cell fate mechanisms can play in influencing mosaic formation.

To date, the best known example of cell fate mechanisms controlling the formation of regular cell spacing in the retina is the lateral inhibition of cell fates in *Drosophila* eye (Frankfort and Mardon, 2002). In this system, several molecular signalling pathways, including Delta-Notch

signalling, determine one cell from a pool of precursor cells to become an R8 photoreceptor. After each R8 cell has been determined, the surrounding cells take on different fates to make a full complement of photoreceptors within an ommatidium. It has recently been suggested (Frankfort and Mardon, 2002) that vertebrate ganglion cell development follows a similar path, given that they are the first cells to be produced, and that they inhibit surrounding cells from also becoming retinal ganglion cells (RGCs), perhaps mediated via Delta-Notch signalling (Austin et al., 1995; Waid and McLoon, 1998). In chick retina, as soon as RGCs are identifiable, they are arranged regularly, although it is not known how many types of RGCs will be formed from this initial population (McCabe et al., 1999). The effects of these lateral inhibition mechanisms upon spatial regularity have not yet been investigated experimentally.

A related issue in retinal development is how complementary types of cells might form. In particular,  $\alpha$  and  $\beta$  RGCs form two complementary types, on- and off-centre, depending on whether the cell responds to onsets or offsets of light. This physiological classification is mirrored by an

anatomical distinction in mature RGCs: the dendrites of on- and off-centre RGCs stratify in different layers of the inner plexiform layer (IPL) (Famiglietti and Kolb, 1976). However, at early stages of development, the dendrites of an RGC initially bistratify into both sublayers of the IPL, before eventually losing dendrites in one sublayer of the IPL (Bodnarenko and Chalupa, 1993). It is still not known whether the on- and off-centre  $\alpha$  (or  $\beta$ ) RGCs are generated independently, or whether a cell first becomes an RGC, then maybe an  $\alpha$  RGC, and finally becomes either an on- or off-centre  $\alpha$  RGC. For example, Jeyarasasingam et al. (Jeyarasasingam et al., 1998) have suggested that on- and off-centre cells may be generated and spatially positioned independently of each other in a random manner, but then postnatal cell death helps improve the regularity of each mosaic by removing inappropriately placed cells. Alternatively, once an initial population of bistratified RGCs has been produced, environmental interactions, such as competition for inputs from bipolar cells, may decide the fate of a ganglion cell to become either on- or off-centre (Kirby and Steineke, 1996). These competing hypotheses for formation of on- and off-centre RGC mosaics have not yet been evaluated in detail.

One approach to studying these various hypotheses for mosaic formation is to use theoretical models to explore the implications of different mechanisms upon development. Several theoretical models of mosaic formation have been produced. Exclusion zone models (where cells are randomly positioned, subject only to the constraint that they do not come within some minimal distance of other cells) have successfully replicated the distribution of retinal mosaics (Galli-Resta et al., 1997; Galli-Resta et al., 1999).  $\beta$  RGC mosaics could also be replicated by assuming each cell is displaced randomly from a regular hexagonal mosaic (Zhan and Troy, 2000). These models capture the statistical properties of the mosaics, but do not explain any particular biological mechanisms. By contrast, models employing more biological mechanisms have recently been produced. The possibility that fish photoreceptors self organise by swapping location with neighbouring cells of different types has been studied theoretically (Mochizuki, 2002). In addition, we have previously investigated the role of dendritic interactions in guiding lateral cell movement underlying the formation of mosaics (Eglén et al., 2000). For a fuller review of modelling in this field, see Eglén et al. (Eglén et al., 2002).

Only Tohya et al. (Tohya et al., 1999) have studied the effects of cell fate upon retinal mosaic formation. In this study, they showed that the spatial arrangement of different types of fish photoreceptor can be generated by allowing the fate of each cell to change according to the fate of neighbouring cells. However, this model assumed that initially cells are initially positioned in a perfect square lattice. This regular geometry may be appropriate for modelling fish photoreceptors, but most retinal mosaics are far less regular than seen for the fish photoreceptors. Even in other models where cell fate has been studied, cells are positioned in regular hexagonal arrays (Goodyear et al., 1995; Collier et al., 1996; von Dassow et al., 2000). To our knowledge, the effect of cell fate upon the spacing of different types of cells in irregular arrays has not been studied, although the effect upon the relative numbers of cells has been investigated (Honda et al., 1990; Tanemura et al., 1991). Our current work therefore extends these previous

approaches by investigating the effects of cell fate mechanisms in irregular arrays. In the first part of this paper, we explore the effect of cell fate processes upon mosaic regularity of both the undifferentiated and differentiated populations. In the second part we compare two mechanisms, cell fate and cell death, to see whether they alone or together are suitable to generate the observed distributions of on- and off-centre RGCs. Some of this work has been previously presented in abstract form (Eglén and Willshaw, 2000).

## MATERIALS AND METHODS

The exclusion zone model was used to create a population of *N* undifferentiated cells (Galli-Resta et al., 1997) of varying regularity. A square region of retinal tissue with area *A* (typically 1 mm<sup>2</sup>) was simulated. Cells were positioned at random within the tissue, subject to the constraint that the distance to the nearest-neighbour was greater than some minimum value,  $d_{\min}$ . The packing intensity,  $\tau$ , of the cells was measured as (Diggle, 1983):

$$\tau = N\pi d_{\min}^2/4A. \quad (1)$$

This reflects the degree to which the surface is covered by non-overlapping discs of diameter  $d_{\min}$ . The expected maximal value for exclusion zone models is around 0.55, compared with 0.91 for a hexagonal arrangement of cells (Diggle, 1983). Values of  $d_{\min}$  were therefore chosen such that the packing intensity was in the range [0,0.5].

### Cell fate mechanisms

Two different styles of simulating cell fate were investigated here, namely a one-step method (Honda et al., 1990) and an iterative method (Collier et al., 1996). Both are lateral inhibitory methods, in which some local process decides whether an initially undifferentiated cell should eventually acquire one of two fates. If the cell fate process is competitive, then typically a cell that wins the competition acquires primary fate, and a cell that loses the competition adopts secondary fate. In the iterative method, each cell continuously updates its decision to acquire primary or secondary fate; by contrast, in the one-step methods, the fate decision is made just once.

In both the one-step and iterative methods, we need to decide which cells compete with each other during the cell-fate process. Here, we assume each cell competes with its neighbours to acquire primary fate. As cells are not positioned in a regular grid across the retinal surface, we have used the Voronoi tessellation (Fortune, 1987) (<http://cm.bell-labs.com/netlib/voronoi/index.html>) to decide whether two cells are neighbours. The Voronoi tessellation divides the retinal surface into non-overlapping polygons, one per cell. The Voronoi polygon of a cell represents the region of space that is closest to that cell (see Fig. 1A, for an example). Two cells are then neighbours of each other if they share an edge of a Voronoi polygon. Rather than suggesting that the retina computes the Voronoi tessellation to discover its neighbours, we simply use it here as a good first approximation as to which cells might communicate with each other during development.

The one-step methods for lateral inhibition of cell fate (Honda et al., 1990; Tanemura et al., 1991) are simpler to implement than the iterative methods. Honda et al. (Honda et al., 1990) devised several related one-step methods, differing in only the ranking technique used. Once an initial undifferentiated population of cells has been created with the exclusion zone model, the Voronoi tessellation (Fortune, 1987) is calculated, and the neighbours of each cell found. The cells are then ranked according to some criterion. Each cell is sequentially selected in order of its rank; if it is undifferentiated, it acquires primary fate and all its neighbours adopt secondary fate. Otherwise, if the cell already has primary or secondary fate, the fate

of the cell is unchanged. Tanemura et al. (Tanemura et al., 1991) investigated four different ranking techniques:

- (1) in order of decreasing Voronoi polygon area (largest)
- (2) in order of increasing Voronoi polygon area (smallest)
- (3) at random (random)
- (4) alternately selecting cells closest to the left and right edge of the tissue (left-right).

To model lateral inhibition in a more realistic way than the one-step methods, we used the iterative method presented by Collier et al. (Collier et al., 1996) to simulate Delta-Notch signalling. In this formulation, the primary and secondary cell fates are represented by high levels of Delta and Notch, respectively. High levels of Delta in one cell induce higher Notch expression in its neighbours, which in turn decreases the expression of Delta in these cells. Consequently, expression of these two factors tends to be driven to opposing extremes. This signalling mechanism is formalised by assuming each cell  $i$  has two variables,  $n_i$  and  $d_i$ , that represent the level of Notch and Delta, respectively. (In this form, each variable is dimensionless and varies between [0,1].) Initially,  $n_i$  and  $d_i$  are chosen from a uniform random distribution in the range [0.9,1]. They are then updated by the following coupled differential equations:

$$\frac{d}{dt} n_i = f(\bar{d}_i) - n_i \quad (2)$$

$$\frac{d}{dt} d_i = g(n_i) - d_i, \quad (3)$$

where  $f()$  and  $g()$  are respectively monotonically increasing and decreasing functions:

$$f(x) = x^2/(a + x^2)$$

$$g(x) = 1/(1 + bx^2).$$

(Typically  $a=0.01$ ,  $b=100$ .)  $\bar{d}_i$  is the average value of  $d$  for cells that are considered neighbours of cell  $i$ . We have used two different methods to decide whether cells are neighbours:

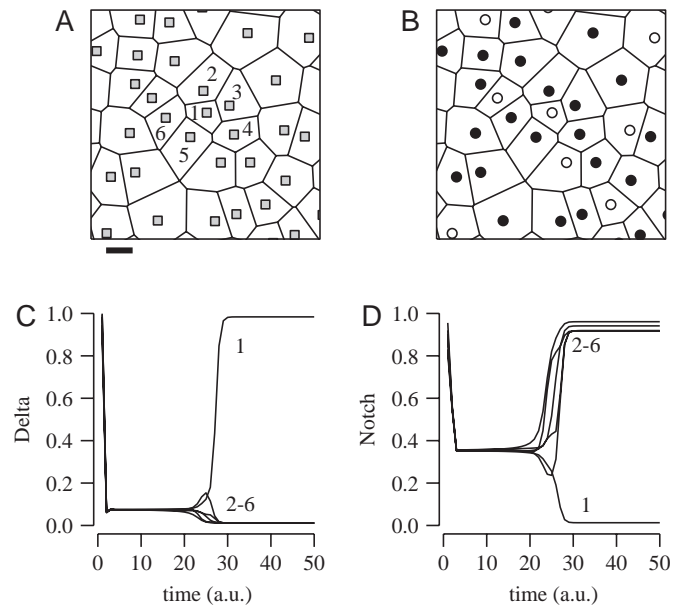
- (1) Compute the Voronoi tessellation of all cell positions; two cells are considered neighbours of each other if their Voronoi polygons share an edge. Typically each cell has five to seven neighbours. This method is called all-neighbours inhibition (ANI).
- (2) Select the cell  $j$  that is closest (as measured by the Euclidean distance between cell positions) to cell  $i$ . In this case, each cell has only one neighbour and so  $\bar{d}_i=d_j$ . This method is called nearest-neighbour inhibition (NNI).

Fig. 1 illustrates the difference in the two types of neighbourhoods. The differential equations [(2) and (3)] were solved numerically until the activity of all cells had reached stable values (see Computational details). At this point, each cell  $i$  acquired primary fate if  $d_i > 0.9$ , otherwise it acquired secondary fate.

### Cell death

The mechanisms that underlie cell death in the retina are not clearly understood. Even in other systems, there are few theoretical models investigating cell death (for a review, see Clarke, 2002). Jeyarasasingam et al. (Jeyarasasingam et al., 1998) suggest that cell death may help mosaic formation by removing those cells that are inappropriately placed. However, this case has not yet been formalised. To allow us to investigate the impact of cell death upon mosaic formation, we investigated three possible mechanisms of cell death. These methods do not correspond to any known biological processes of cell death, but allow us to begin to investigate the importance of cell death in mosaic formation. When choosing which cell should die, one of three methods was used.

- (1) Distance: delete the cell with the smallest nearest-neighbour distance.
- (2) Area: delete the cell with the smallest Voronoi polygon area.



**Fig. 1.** Example of lateral inhibition among a small group of cells. (A) Sample of undifferentiated cells (grey squares) created with the exclusion zone model ( $d_{\min}=15.96 \mu\text{m}$ ,  $\tau=0.2$ ;  $A=1 \text{ mm}^2$ ;  $N=1000$ ). Six central cells are numbered for plots in (C,D). Scale bar:  $20 \mu\text{m}$ . In this case, all-neighbours inhibition (ANI) was used, so cell 1 has five neighbouring cells (labelled 2-6). By contrast, cell 3 has six neighbours, because its Voronoi polygon has six edges. If nearest-neighbour inhibition (NNI) was used, cell 1 would have just one neighbour (cell 2). (B) The same cells once the levels of Delta and Notch have stabilised. Open circles denote primary fate cells, filled circles are secondary fate cells. Cell 1 acquires primary fate, cells 2-6 adopt secondary fate. (C,D) The levels of Delta and Notch during development for the six cells highlighted in A. Time is measured in arbitrary units (a.u.).

- (3) Random: delete a cell at random.

If more than one cell shares the same minimum distance or Voronoi polygon area, one of those cells is randomly selected to die. Also, for methods 1 and 2, once a cell has been deleted, the nearest-neighbour distances and Voronoi polygon areas are recalculated for the remaining cells.

Cells are deleted one by one until a fixed percentage of cells have been deleted. Up to 20% of  $\alpha$  ganglion cells may die postnatally (Jeyarasasingam et al., 1998), although here we have tested the effects of up to 40% cell death. When investigating the role of cell death upon the formation of on- and off-centre RGC mosaics, cells were deleted independently from each mosaic.

### Evaluating mosaic regularity

Mosaic regularity was evaluated with two complementary measures. The regularity index is the ratio of the mean to the standard deviation of the distances from each cell to its nearest-neighbour of the same type (Wässle and Riemann, 1978). The higher the regularity index, the more regular the mosaic; values greater than 2 typically indicate a non-random distribution (Cook, 1996). The second measure is the packing factor (Rodieck, 1991), which quantifies how well a set of disks of a given radius are packed. The packing factor ranges from 0 for a random distribution to 1 for a perfectly hexagonal arrangement. The formulae required for computing the packing factor are more detailed than the regularity index; full details are given by Rodieck (Rodieck, 1991). Packing factors were calculated using 20 bins, each  $5 \mu\text{m}$  wide. Experimentally observed retinal mosaics typically have

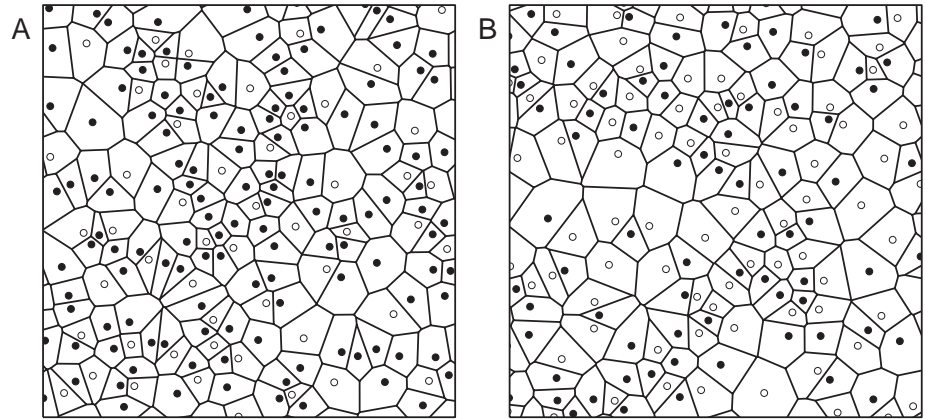


**Fig. 2.** Example outcomes of the all-neighbours and nearest-neighbour inhibition methods. Scale bar: 100  $\mu\text{m}$ . In each plot, only a central region of the simulated retina is shown. (A) An initial population of 1000 cells was created using the exclusion zone model ( $d_{\text{min}}=11.28 \mu\text{m}$ ,  $\tau=0.1$ ;  $A=1 \text{ mm}^2$ ;  $N=1000$ ). All-neighbours inhibition (ANI) then transformed this population into primary (open circles) and secondary fate (filled circles) cells. Here, the cell count ratio is 2.64:1. (B) As in A, but using nearest-neighbour inhibition (NNI). Here, the cell count ratio is 1.06:1.

regularity indexes of 4-9, with packing factors around 0.1-0.4. Both the regularity index and packing factor are dimensionless. For the cell fate mechanisms, we also measured the cell count ratio: the number of secondary fate cells divided by the number of primary fate cells.

### Computational details

When computing the Voronoi tessellation (Fortune, 1987), toroidal wraparound conditions were imposed so that cells at the borders were considered neighbours of each other. This was done so that each cell had roughly an equal number of neighbours. When computing the regularity index, we measured the nearest-neighbour distance of cells within the central region (all cells that were not within 100  $\mu\text{m}$  of an edge). Any artifacts introduced by the toroidal wraparound were reduced using this technique. For the packing factor measurement, we ignored all cells within 100  $\mu\text{m}$  of an edge, and instead used the correction factor suggested by Rodieck (Rodieck, 1991) to handle edge effects.

The system of 2N differential equations given by (2) and (3) were solved numerically using the ordinary differential equation solver LSODE from Octave ([www.octave.org](http://www.octave.org)). This system has an unstable homogeneous steady state (when all Notch levels are equal, and all Delta levels are equal), as seen during times 5-20 in Fig. 1C,D. Any small perturbation of this steady state then self amplifies into one of two stable inhomogeneous steady states (Collier et al., 1996) when a cell is driven to have high Delta activity and low Notch activity (or vice versa; seen in Fig. 1C,D for times beyond 30). Hence, the simulations were run until the network reached the stable inhomogeneous steady state.

Computer simulations and analysis were performed in Octave and R (Ihaka and Gentleman, 1996). To test the robustness of the models, each simulation was run repeatedly from different initial conditions by generating different initial cell positions in the exclusion zone model. The simulations are summarised here by plotting error bars denoting the mean  $\pm 1$  s.d. of each measure. Some error bars are smaller than the symbol depicting the mean, and hence are not visible.

## RESULTS

Fig. 1 shows an example of all-neighbours inhibition among a small number of cells. The undifferentiated population divides into a small group of primary fate cells and a larger group of secondary fate cells. As the competition is restricted to its Voronoi neighbours, as one cell gets high Delta levels (cell 1), all the surrounding cells (cells 2-6) get high Notch activation. Ultimately, cell 1 takes on primary fate, and its neighbours (cells 2-6) adopt secondary fate. The effect of this

mechanism upon a larger population of initial undifferentiated cells is shown in Fig. 2A. Each primary fate cell is surrounded by secondary fate cells. By contrast, when the lateral inhibition is restricted to nearest-neighbour only, as in Fig. 2B, we typically see an equal number of primary and secondary fate cells.

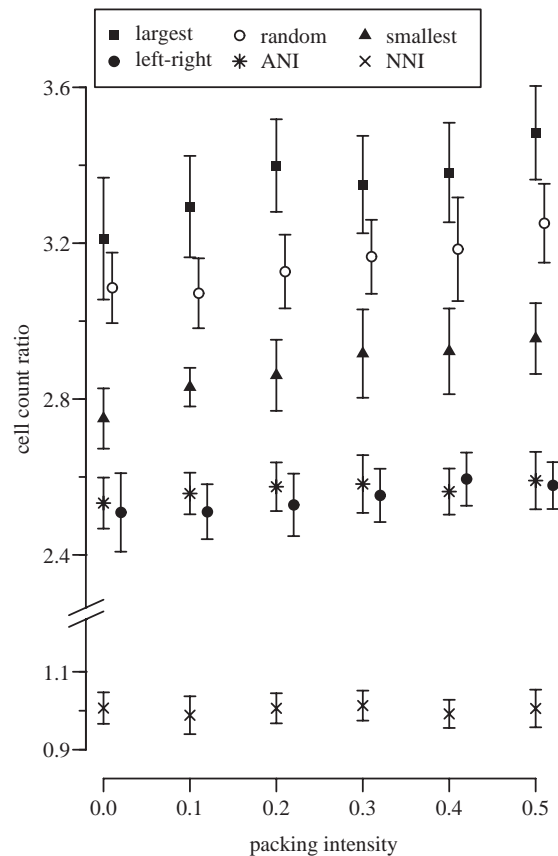


**Fig. 3.** Effect of packing intensity upon the cell count ratio for different cell fate methods. For each of the six packing intensities tested, 20 simulations for each cell fate method were run from different initial populations created using the exclusion zone model ( $A=1 \text{ mm}^2$ ;  $N=1000$ ). The symbols for the random and left-right methods have been shifted horizontally so that symbols do not overlap.

**Cell count ratio**

Given that each cell typically has five to seven Voronoi neighbours, and that each secondary fate cell typically, but not always, has two primary fate neighbours, the estimated cell count ratio is expected to be 2.5-3.5:1. The cell count ratio was measured for the different cell fate mechanisms (Fig. 3). For the one-step mechanisms, our results agreed with previous work (Honda et al., 1990; Tanemura et al., 1991): for a given packing intensity, the cell count ratio was highest for the largest method, and lower for the smallest method. This is expected, as the area and number of edges of a Voronoi polygon are positively correlated [see Fig. 6 by Tanemura et al. (Tanemura et al., 1991)]. Hence, if cells with larger polygon areas are picked first, they will influence a high number of neighbouring cells to acquire secondary fate. The random method produced cell count ratios around 3:1, in between the largest and smallest method. The left-right method and all-neighbours inhibition produced similar cell count ratios, typically around 2.6:1. By contrast, nearest-neighbour inhibition produced cell count ratios around 1:1. This is as expected as the cells usually, but not always, compete with just one other cell, and so for every primary fate cell, there will typically be one secondary fate cell.

To test whether the packing intensity,  $\tau$ , of the initial undifferentiated population influenced the cell count ratio, we compared the cell count ratio when  $\tau=0.0$  with  $\tau=0.5$  for each

cell fate method using the two-sample Wilcoxon test. For the largest, smallest and random one-step methods, the cell count ratio was significantly higher when  $\tau=0.5$  than when  $\tau=0.0$  ( $P < 10^{-6}$  in each case). This trend was weaker, but still significant, for the left-right method ( $P=0.023$ ) and for all-neighbours inhibition ( $P=0.01$ ). Finally, there was no increase in cell count ratio with packing intensity for the nearest-neighbour inhibition method ( $P=0.90$ ). Hence, the cell count ratio is less sensitive to variations in  $\tau$  for the iterative than the one-step methods.

**Regularity index and packing factor**

The effects of the different cell fate mechanisms upon the regularity index of the mosaics are summarised in Fig. 4. All four one-step mechanisms and the all-neighbours inhibition produced similar effects upon the regularity index. When the packing intensity of the undifferentiated mosaic was small, the regularity of the primary fate mosaic was higher than the regularity of both the undifferentiated and secondary fate mosaics. Hence, cell fate mechanisms can produce a regular primary fate, but not secondary fate, mosaic from an irregular array of undifferentiated cells. However, once the packing intensity of the undifferentiated mosaic exceeded a critical value ( $\tau=0.3-0.4$ ), the regularity of both primary and secondary fate mosaics was always less than the regularity of the undifferentiated mosaic. With one exception ( $\tau=0.5$  in the

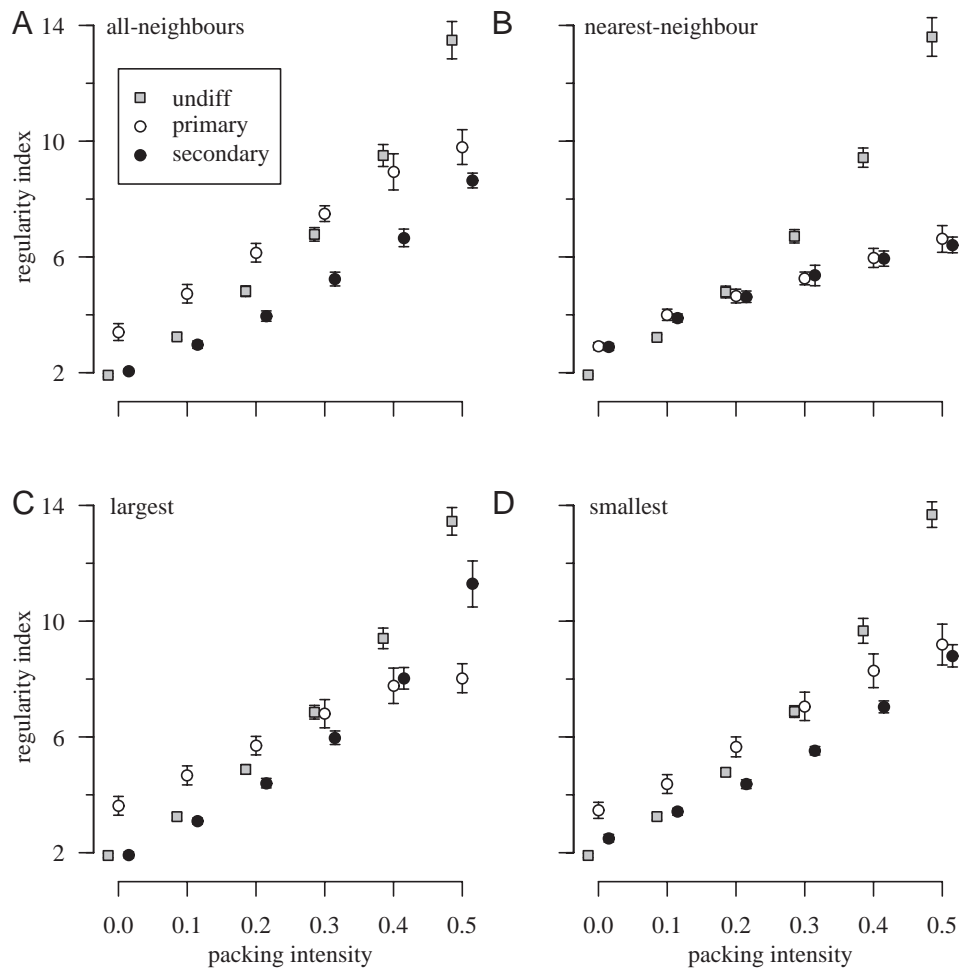


**Fig. 4.** Regularity index of the mosaics of undifferentiated cells, and subsequent primary and secondary fate cells, as a function of packing intensity of the undifferentiated mosaic. This figure summarises the same simulations as described in Fig. 3. The symbols for undifferentiated and secondary fate cells have been horizontally shifted slightly so that symbols do not overlap. (A) Effect of all-neighbours inhibition upon the regularity index. (B) Effect of nearest-neighbour inhibition. (C) Effect of the largest one-step method. (D) Effect of the smallest one-step method. The effects of random and left-right methods were similar to C,D and so are not shown here.

largest method), the primary fate mosaic was always more regular than the secondary fate mosaic. Therefore, if the initial population of undifferentiated cells is already regular, cell fate produces less regular primary and secondary fate mosaics.

The behaviour of nearest-neighbour inhibition was slightly different (Fig. 4B). First, regardless of packing intensity, the regularity of primary and secondary fate mosaics was always similar. For low packing intensities ( $\tau=0.0-0.1$ ), both primary and secondary fate mosaics were more regular than the undifferentiated mosaic. Second, the critical value of packing intensity at which undifferentiated mosaics were more regular than both primary and secondary fate mosaics was lower (typically when  $\tau=0.2$ ) than the threshold for the other cell fate mechanisms.

The effect of packing intensity upon the packing factor (Rodieck, 1991) of the undifferentiated, primary fate and secondary fate mosaics was similar to the effect upon the regularity index (Fig. 5). At low packing intensities, the packing factor of the primary fate mosaic was higher than both the undifferentiated and secondary fate mosaic. Once the packing intensity exceeded some critical value, the undifferentiated mosaic had a higher packing factor than either the primary or secondary fate mosaic. Again, this critical value was lower for nearest-neighbour inhibition ( $\tau=0.2-0.3$ ) than the other methods ( $\tau=0.4-0.5$ ).

### On- and off-centre mosaics

Some populations of retinal cells can naturally be divided into two complementary types of roughly the same number of cells. The best known examples are probably the classification of  $\alpha$  and  $\beta$  RGCs into on- and off-centre types (Wässle et al., 1981a; Wässle et al., 1981b). Could such mosaics be generated from an initial bistratified population simply by cell fate? Out of the cell fate mechanisms tested here, only nearest-neighbour inhibition produced cell count ratios around 1:1, matching those observed experimentally (Table 1). However, by comparing the regularity index of the experimental mosaics (Table 1) with the results from nearest-neighbour inhibition, we have shown it to be unlikely that lateral inhibition alone is sufficient to generate the spatial distributions observed in adult. By contrast, the regularity indexes measured from the cholinergic amacrine cells (Diggle, 1986) are closer to those produced by nearest-neighbour inhibition with a packing intensity of 0.1. It is therefore unlikely that cell fate mechanisms alone are responsible for generating the adult distributions of on- and off-centre RGCs from a random undifferentiated population.

### Cell death and mosaic formation

The results from the previous section indicate that lateral inhibition of cell fate alone cannot generate the pattern of on- and off-centre RGC mosaics from an irregular population of

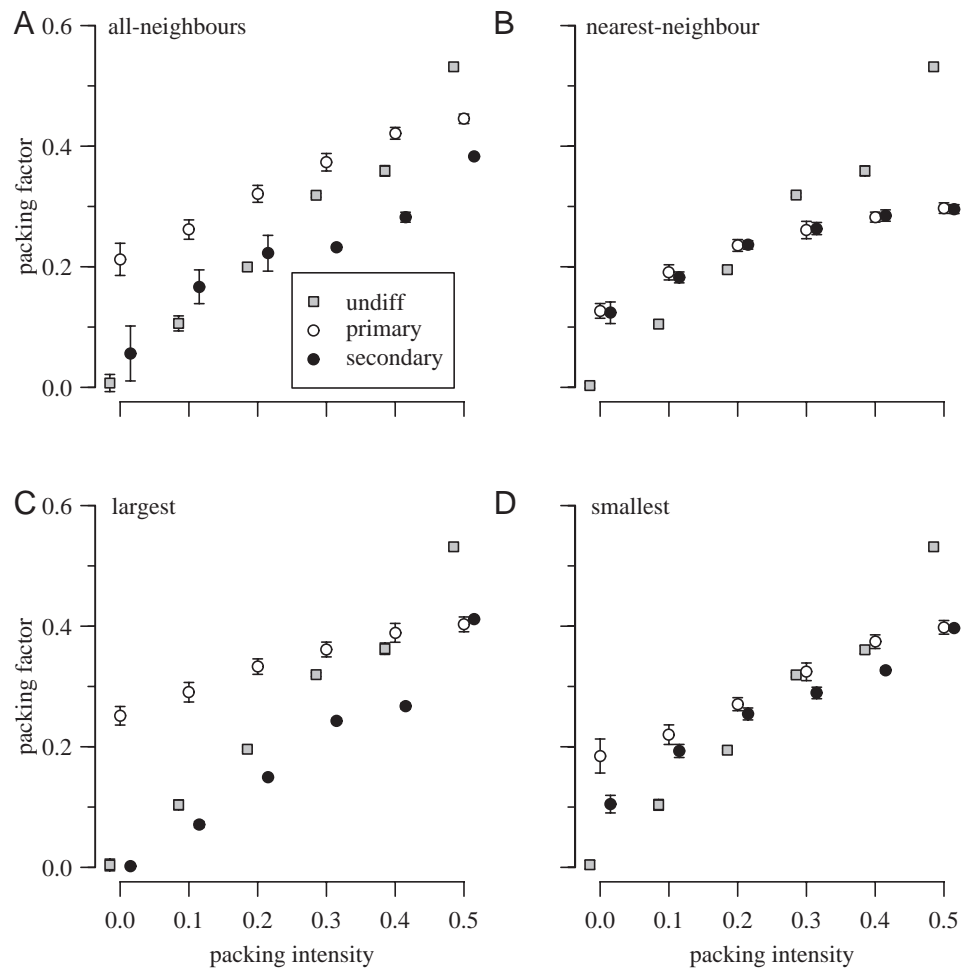


**Fig. 5.** Packing factor of the mosaics of undifferentiated cells, and subsequent primary and secondary fate cells, as a function of packing intensity of the undifferentiated mosaic. This figure summarises the same simulations as described in Fig. 3 with the same conventions as Fig. 4.

**Table 1. Regularity of several on- and off-centre types of retinal cells**

Cell type	Reference	On/off	Regularity index		
			On+off	On	Off
Cat $\alpha$ RGC	Wässle et al., 1981a	0.83	2.4	4.5	4.7
Cat $\beta$ RGC	Wässle et al., 1981b	0.92	2.7	5.3	5.3
Rabbit cholinergic AC	Diggle, 1986	1.07	2.8	3.5	3.9

On/off is defined here as the number of on-centre cells divided by the number of off-centre cells. The regularity index of  $\alpha$  and  $\beta$  retinal ganglion cell (RGC) mosaics were taken from the references. The regularity indexes for the cholinergic amacrine cells (AC) of the rabbit were not reported by Diggle (Diggle, 1986), and so were calculated for the current study. Cell count ratios and regularity indexes from Jeyarasasingam et al. (Jeyarasasingam et al., 1998) were not given, although their paper suggests the regularity of either on- and off-centre  $\alpha$  RGCs in adult cat is around 4.0.

bistratified RGCs. Recent experimental findings suggest that the pattern of on- and off-centre  $\alpha$ -RGCs in the cat could be sculpted by postnatal cell death, and that the pattern, but not the magnitude, of this cell death is activity dependent (Jeyarasasingam et al., 1998). From these results, the authors suggested that 20% cell death is sufficient to transform irregular mosaics into the regular adult pattern. To support this claim, cells were deleted from computer-generated random mosaics and shown to match the adult pattern. However, the deleted cells were chosen by eye, rather than by following any rules (Leo Chalupa, personal communication). Hence, to test this hypothesis, we needed to test simple rules for choosing which cells to die from a random population.

Fig. 6 shows the results of using three methods of cell death upon mosaic regularity. Unsurprisingly, the distance method produces the mosaics with the highest regularity – at each step we are simply removing the smallest value from the distribution of nearest-neighbour distances. Deleting cells according to their Voronoi area also improves the regularity index, but to a lesser degree than deleting by distance ( $P=0.007$  after 20% cells deleted;  $P<0.001$  after 40% cells deleted; both tests two-sample Wilcoxon test). However, when regularity is assessed using the packing factor, deleting cells by the area

method produces more regular mosaics than the distance method ( $P=0.035$  after 20% cells deleted;  $P<0.001$  after 40% cells deleted; both tests two-sample Wilcoxon test). By contrast, deleting cells simply at random does not improve mosaic regularity, as assessed by both the regularity index and packing factor.

Fig. 6 also demonstrates that the regularity index and the packing factor measure different aspects of mosaic regularity, as the two measures are not perfectly correlated. If the two measures were highly correlated, we would expect that the cell death method that maximises the packing factor also maximises the regularity index. However, Fig. 6 shows that the regularity index is maximised by deleting cells according to nearest-neighbour distance, whereas the packing factor is maximised by deleting cells according to their Voronoi area. This result is unsurprising, as the regularity index measures the distance of each cell to only its nearest-neighbour, whereas the packing factor measures the distance to many neighbouring cells, as it is based on the autocorrelation of cell positions. However, the data in Fig. 6 are based upon deletions from simulated mosaics. The degree of correlation between regularity index and packing factor may be better tested upon real mosaics, similar to the way the correlation between regularity index and dispersion index was investigated [see Fig. 6B by Cook (Cook, 1996)].

To test whether cell death is sufficient to create the spatial distribution of on- and off-centre ganglion cells, three related hypotheses were examined concerning how the on- and off-centre mosaics might arise, before any cells then die. The first hypothesis (independence) was suggested by Jeyarasasingam et al. (Jeyarasasingam et al., 1998): on- and off-centre cells are generated independently in a random distribution. The second hypothesis (random division), suggested by Cook and Chalupa (Cook and Chalupa, 2000), is that there is an initial population of bistratified RGCs which presumably form an irregular mosaic. Each RGC then randomly decides to become either on- or off-centre. The third hypothesis (inhibition), also suggested by Cook and Chalupa (Cook and Chalupa, 2000), is like the random division hypothesis, except that neighbouring RGCs tend to become opposite types, rather than being assigned on-

**Fig. 6.** Effect of different cell death methods upon the regularity index and packing factor of the mosaics. An initial mosaic of 400 cells was created using the exclusion zone model ( $d_{\min}=10\ \mu\text{m}$ ,  $\tau=0.008$ ;  $A=4\ \text{mm}^2$ ). Cells were removed one-by-one until 40% of cells had been deleted. Starting with the same initial mosaic, all three methods (selecting cells either by smallest Voronoi area, smallest nearest-neighbour distance or at random) were tested. Hence the results for 0% cell death (showing the initial regularity) are the same for each method. Ten different initial mosaics were created, from which the mean and s.d. of the regularity index were calculated for each method.

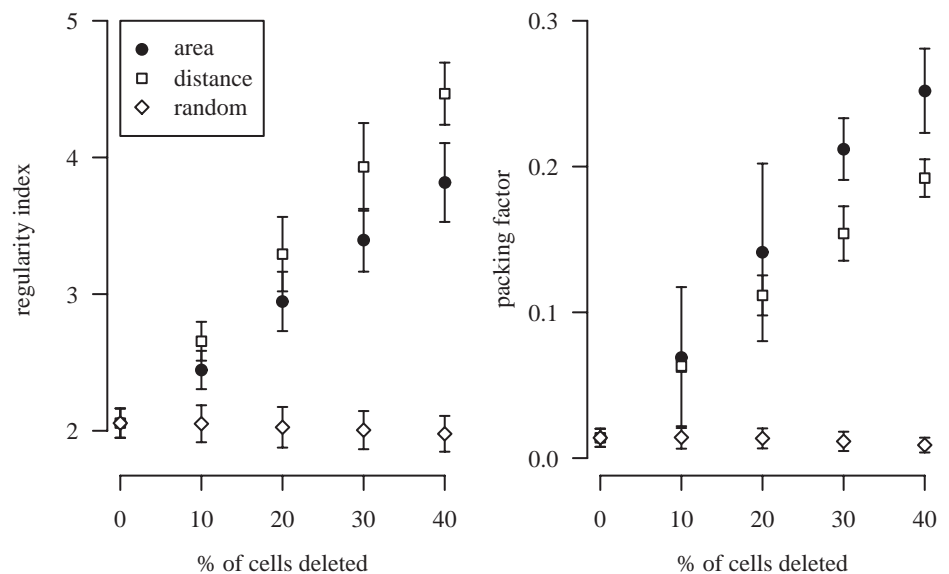
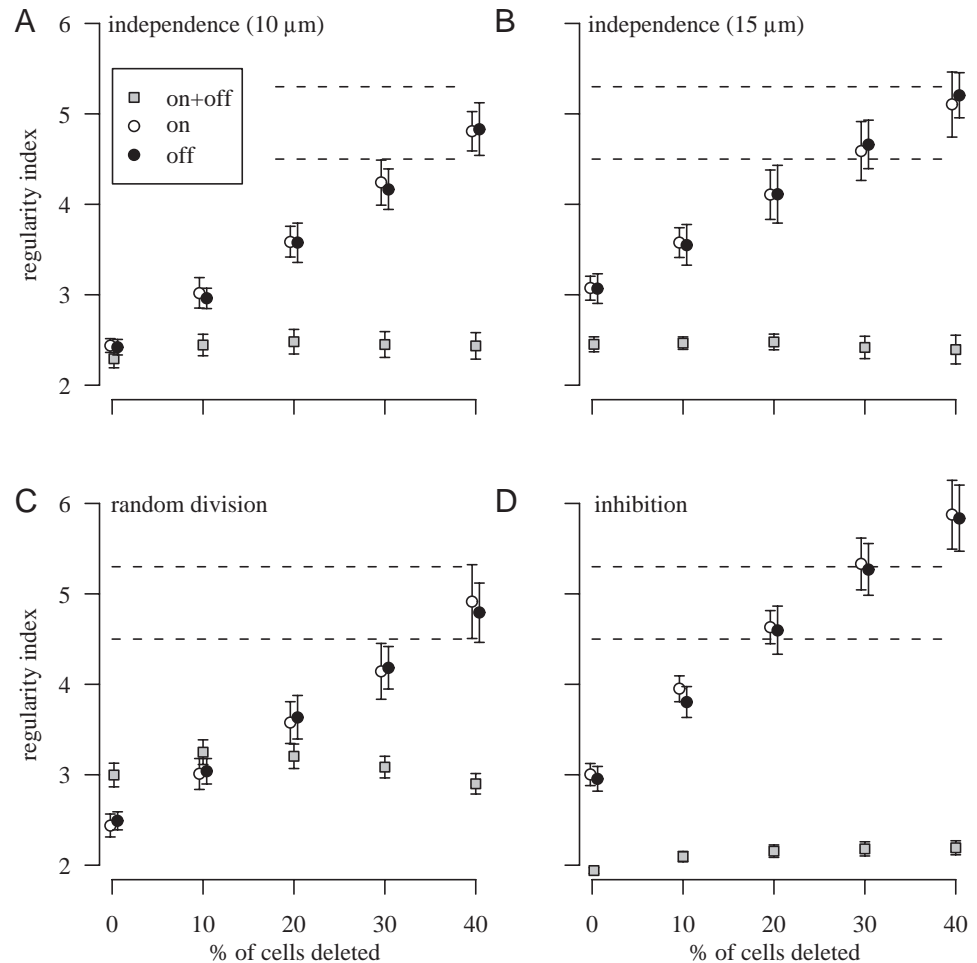


**Fig. 7.** Evaluation of hypotheses for formation of on- and off-centre RGC mosaics. (A) Initial populations of 500 on-centre and 500 off-centre cells were created independently using the exclusion zone model ( $d_{\min}=10\ \mu\text{m}$ ,  $\tau=0.04$ ;  $A=1\ \text{mm}^2$ ). Up to 40% of cells were deleted (using the distance method) independently from each population. The mean and s.d. of the regularity index over ten simulations, with different initial conditions, are plotted for just the on- or off-centre cells (open or filled circles) and for the combined population of on- and off-centre cells (grey squares). Broken lines show the range of regularity indexes for the on- or off-centre RGCs, from Table 1. (B) Same as A, but  $d_{\min}=15\ \mu\text{m}$  ( $\tau=0.09$ ). (C) As in A, but an initial population of 1000 cells was created using the exclusion zone model ( $d_{\min}=10\ \mu\text{m}$ ,  $\tau=0.08$ ) and then divided into on- and off-centre subpopulations by randomly assigning each cell to one of two types. (D) As in A, but an initial population of 1000 cells was created using the exclusion zone model ( $d_{\min}=0\ \mu\text{m}$ ,  $\tau=0$ ) and divided into on- and off-centre subpopulations by nearest-neighbour inhibition (NNI). The  $d_{\min}$  value in B was chosen so that the regularity of the on- and off-centre mosaics were similar to those in D before cell death.



or off-centre at random. To implement this hypothesis, we used nearest-neighbour inhibition, and arbitrarily assume that primary fate cells become on-centre, and secondary fate cells become off-centre. Hence, the independence hypothesis suggests that on- and off-centre RGCs are generated independently of each other, whereas the random division and inhibition hypotheses state that the on- and off-centre cells are produced by subdivision from some initial population of bistratified RGCs. For each hypothesis, once the on- and off-centre populations were created, up to 40% of cells from each population were then killed using the distance cell death method.

The consequences of these hypotheses are shown in Fig. 7. Under the independence hypothesis, 20% cell death linearly increases the regularity of both on- and off-centre RGC mosaics from around 2.5 to 3.6 (Fig. 7A). To produce regularity indexes matching those found experimentally (Table 1), typically up to 40% cell death is required. The final regularity index of each mosaic is of course dependent on the regularity of the initial populations of on- and off-centre cells. If the initial populations of on- and off-centre cells is mildly regular (Fig. 7B), less cell death, typically 30%, is required to match the experimental regularity indexes. However, this somewhat defeats the purpose: the aim was to transform an irregular distribution to a regular distribution, rather than to start with a regular distribution.

The random division hypothesis produced similar results (Fig. 7C). Given an initial undifferentiated population of low regularity, randomly assigning each cell as on- or off-centre produces two irregular mosaics. Cell death does improve the regularity of each mosaic, but in a similar pattern to that seen in Fig. 7A.

By contrast, under the inhibition hypothesis (Fig. 7D), even if the initial population of bistratified RGCs is irregular, lateral inhibition produces mildly regular mosaics, similar in regularity to those created in Fig. 7B (compare data points in B,D before any cell death). Furthermore, the rate at which regularity increases per cells deleted is highest under the inhibition hypothesis, such that 20–30% cell death produces mosaics with regularity indexes matching those found experimentally (Table 1).

## DISCUSSION

This paper has presented two main results concerning the potential influence of cell fate upon the formation of retinal mosaics. First, we have demonstrated that cell fate mechanisms can produce a regular distribution of primary fate cells from an irregular undifferentiated population. If cell fate interactions are restricted to pairs of cells (as nearest-neighbour inhibition is), then the secondary fate mosaic is

typically as regular as the primary fate mosaic. Otherwise, the secondary fate mosaic tends to be slightly less regular than the initial undifferentiated population. However, if the initial undifferentiated population is already regular (with a regularity index above 5-6), the primary fate mosaic is no more regular than the population from which it came. Second, we have applied these cell fate mechanisms to the specific problem of the formation of on- and off-centre RGC mosaics. Neither cell fate nor cell death alone can transform an irregular population into the observed on- and off-centre RGC mosaics. However, we suggest that an initial undifferentiated population can divide into mildly regular on- and off-centre populations from which cell death increases the regularity to experimentally observed levels.

The results may be somewhat sensitive to the exact nature of the cell fate mechanism. However, we achieved similar results for several one-step mechanisms (Honda et al., 1990) and an iterative mechanism (Collier et al., 1996), indicating the results are somewhat robust. The main difference between the cell fate methods tested here is that the one-step methods tend to have a higher ratio of secondary to primary fate cells. One-step methods may also be more prone to 'fractures', whereby two neighbouring cells acquire primary fate if more than one initiation site is used (Goodyear et al., 1995).

In principle then, cell fate mechanisms, perhaps mediated by Delta-Notch signalling, could produce a regular array of early differentiating cells from an undifferentiated population (Frankfort and Mardon, 2002). However, without knowledge of the regularity of the initial population of undifferentiated cells, detailed comparisons with the early regularity observed in chick RGCs (McCabe et al., 1999) are not possible. However, given the high regularity index of these early differentiating RGCs (around 5.0), our results would suggest that either the initial population must be mildly regular (around 3.0 to produce a primary fate population of 5.0, see Fig. 4A when  $\tau=0.1$ ) or that the cell fate mechanism involves interactions among cells that are not all immediate neighbours. Furthermore, when comparing the regularity of mosaics produced by nearest-neighbour inhibition with on- and off-centre RGCs, we conclude that cell fate alone is unable to account for their regular arrangement. Cell death alone (Jeyarasasingam et al., 1998) also cannot replicate the on- and off-centre RGC patterns, unless cell death is much higher than the 20% reported in postnatal cat. However, the cell fate and cell death mechanisms can be used together to transform one irregular mosaic into two regular mosaics, with regularity indexes similar to those observed experimentally.

The development of the on- and off-centre ganglion cells remains a mystery. Our work here suggests that competition between neighbouring RGCs (Kirby and Steineke, 1996) is insufficient by itself to replicate the mature pattern of RGC mosaics. However, we have shown here that another mechanism, cell death, could follow after lateral inhibition to produce the adult regularity. This suggests that environmental factors are sufficient to determine the fate (on- or off-centre in this case) of RGCs. However, the existence of early recognition between same-centre RGCs raises the possibility that these cells are molecularly distinct from an early age, and so may never be part of the same undifferentiated population (Lohmann and Wong, 2001). In addition, in most species [except rat (see Peichl, 1991)], there are slightly more off-

centre than on-centre  $\alpha$ -cells (Table 1). Such a bias towards more off-centre cells is not explainable in this model, as cell count ratios were typically around 1:1 for nearest-neighbour lateral inhibition.

The models presented in this paper allow us to assess the relative influence of cell fate and cell death upon mosaic formation. However, these mechanisms are somewhat simplistic still, especially concerning cell death. Theoretical models of developmental cell death are still relatively simple (Clarke, 2002) and are an area for future research. We have used simple mechanisms that probably overestimate the influence that cell death can have upon mosaic formation. However, particularly if they are overestimates, the results still show that 20% cell death alone (Fig. 7B,C) is insufficient to generate regular mosaics. Future cell death mechanisms could be based upon competition for neurotrophic resources from presynaptic cells, such that cells receiving insufficient resources are more likely to die. In addition, cell death is unlikely to be a universal method for improving regularity. In postnatal rat, cell death among cholinergic amacrine cells is not thought to affect mosaic regularity (Galli-Resta and Novelli, 2000). Note also that most retinal cell death occurs earlier in development, before the period of mosaic formation, and is suggested instead to relate to the formation of connections in the target area of the RGC axons (O'Leary et al., 1986).

We have limited ourselves to communication between nearest-neighbouring cells. Lateral inhibition could also involve interactions between non-neighbouring cells, perhaps mediated by the filopodia or cytonemes observed in some developing systems (Bryant, 1999). In this paper, we have concentrated on modelling formulations proposed for Delta-Notch signalling, which seems appropriate given experimental evidence (Austin et al., 1995). Future work could incorporate other types of cell communication to see their effect on mosaic formation.

Another limitation is that when comparing the simulated mosaics with experimental data, we have used only the simplest of measures, the regularity index. More sensitive measures, such as those based on distributions of Voronoi polygon area, have recently been used when comparing model and simulated mosaics (Galli-Resta et al., 1999; Zhan and Troy, 2000). However, in those cases the models were phenomenological, rather than mechanistic, as the models were not testing specific biological mechanisms. It is unlikely that the models presented here exactly replicate the spatial distributions observed experimentally (such as those referenced in Table 1) for two reasons. First, we have looked at the role of just two mechanisms, cell fate and cell death, and ignored others, such as lateral migration and non-uniform retinal growth, which may also be involved to produce the overall distribution. Second, the ideal experimental comparison would be against tissue early in development, rather than adult tissue. Unfortunately, the lack of distinct molecular markers for on- and off-centre ganglion cells makes it difficult to collect such data, either early in development or at maturity.

Thanks to Julian Budd, Tim Holy, Ben Reese and Rachel Wong for constructive comments on this manuscript. This work was supported by funding from the Wellcome Trust.

## REFERENCES

- Austin, C. P., Feldman, D. E., Ida, J. A. and Cepko, C. L. (1995). Vertebrate retinal ganglion cells are selected from competent progenitors by the action of Notch. *Development* **121**, 3637-3650.
- Bodnarenko, S. R. and Chalupa, L. M. (1993). Stratification of on and off ganglion cell dendrites depends on glutamate mediated afferent activity in the developing retina. *Nature* **364**, 144-146.
- Bryant, P. J. (1999). Filopodia: fickle fingers of cell fate? *Curr. Biol.* **9**, R655-R657.
- Clarke, P. G. H. (2002). Models of neuronal death in vertebrate development: from trophic interactions to network roles. In *Modeling Neural Development* (ed. A. van Ooyen). Cambridge, MA: MIT Press (in press).
- Collier, J. R., Monk, N. A. M., Maini, P. K. and Lewis, J. H. (1996). Pattern formation by lateral inhibition with feedback: a mathematical model of Delta-Notch intracellular signalling. *J. Theor. Biol.* **183**, 429-446.
- Cook, J. E. (1996). Spatial properties of retinal mosaics: an empirical evaluation of some existing measures. *Vis. Neurosci.* **13**, 15-30.
- Cook, J. E. and Chalupa, L. M. (2000). Retinal mosaics: new insights into an old concept. *Trends Neurosci.* **23**, 26-34.
- Diggle, P. J. (1983). *Statistical Analysis of Spatial Point Patterns*. Academic Press.
- Diggle, P. J. (1986). Displaced amacrine cells in the retina of a rabbit: analysis of a bivariate spatial point pattern. *J. Neurosci. Methods* **18**, 115-125.
- Eglén, S. J. and Willshaw, D. J. (2000). Estimating the influence of cell fate, mediated by lateral inhibition, upon the development of retinal mosaics. *Eur. J. Neurosci.* **12 Suppl.** **11**, 486.
- Eglén, S. J., van Ooyen, A. and Willshaw, D. J. (2000). Lateral cell movement driven by dendritic interactions is sufficient to form retinal mosaics. *Network: Comput. Neural Syst.* **11**, 103-118.
- Eglén, S. J., Galli-Resta, L. and Reese, B. E. (2002). Theoretical models of retinal mosaic formation. In *Modeling Neural Development* (ed. A. van Ooyen). Cambridge, MA: MIT Press (in press).
- Famiglietti, E. V. and Kolb, H. (1976). Structural basis for ON- and OFF-center responses in retinal ganglion cells. *Science* **194**, 193-195.
- Fortune, S. J. (1987). A sweepline algorithm for Voronoi diagrams. *Algorithmica* **2**, 153-172.
- Frankfort, B. J. and Mardon, G. (2002). R8 development in the drosophila eye: a paradigm for neural selection and differentiation. *Development* **129**, 1295-1306.
- Galli-Resta, L. and Novelli, E. (2000). The effects of natural cell loss on the regularity of the retinal cholinergic arrays. *J. Neurosci.* **20:RC60**, 1-5.
- Galli-Resta, L., Novelli, E., Kryger, Z., Jacobs, G. H. and Reese, B. E. (1999). Modelling the mosaic organization of rod and cone photoreceptors with a minimal-spacing rule. *Eur. J. Neurosci.* **11**, 1461-1469.
- Galli-Resta, L., Resta, G., Tan, S.-S. and Reese, B. E. (1997). Mosaics of Islet-1-expressing amacrine cells assembled by short-range cellular interactions. *J. Neurosci.* **17**, 7831-7838.
- Goodyear, R., Holley, M. and Richardson, G. (1995). Hair and supporting-cell differentiation during the development of the avian inner ear. *J. Comp. Neurol.* **351**, 81-93.
- Honda, H., Tanemura, M. and Yoshida, A. (1990). Estimation of neuroblast numbers in insect neurogenesis using the lateral inhibition hypothesis of cell differentiation. *Development* **110**, 1349-1352.
- Ihaka, R. and Gentleman, R. (1996). R: a language for data analysis and graphics. *J. Comput. Graph. Stat.* **5**, 299-314.
- Jeyarasasingam, G., Snider, C. J., Ratto, G. M. and Chalupa, L. M. (1998). Activity-regulated cell death contributes to the formation of on and off alpha ganglion cell mosaics. *J. Comp. Neurol.* **394**, 335-343.
- Kirby, M. A. and Steineke, T. C. (1996). Morphogenesis of retinal ganglion cells: a model of dendritic, mosaic, and foveal development. *Perspect. Dev. Neurobiol.* **3**, 177-194.
- Lohmann, C. and Wong, R. O. L. (2001). Cell-type specific dendritic contacts between retinal ganglion cells during development. *J. Neurobiol.* **48**, 150-162.
- McCabe, K. L., Gunther, E. C. and Reh, T. A. (1999). The development of the pattern of retinal ganglion cells in the chick retina: mechanisms that control differentiation. *Development* **126**, 5713-5724.
- Mochizuki, A. (2002). Pattern formation of cone mosaic in zebrafish retina: a cell rearrangement model. *J. Theor. Biol.* **215**, 345-361.
- O'Leary, D. D. M., Fawcett, J. W. and Cowan, W. M. (1986). Topographic targeting errors in the retinocollicular projection and their elimination by ganglion cell death. *J. Neurosci.* **6**, 3692-3705.
- Peichl, L. (1991). Alpha ganglion cells in mammalian retinae: common properties, species differences, and some comments on other ganglion cells. *Vis. Neurosci.* **7**, 155-169.
- Reese, B. E., Harvey, A. R. and Tan, S.-S. (1995). Radial and tangential dispersion patterns in the mouse retina are cell-class specific. *Proc. Natl. Acad. Sci. USA* **92**, 2494-2498.
- Rodieck, R. W. (1991). The density recovery profile: a method for the analysis of points in the plane applicable to retinal studies. *Vis. Neurosci.* **6**, 95-111.
- Tanemura, M., Honda, H. and Yoshida, A. (1991). Distribution of differentiated cells in a cell sheet under the lateral inhibition rule of differentiation. *J. Theor. Biol.* **153**, 287-300.
- Tohya, S., Mochizuki, A. and Iwasa, Y. (1999). Formation of cone mosaic of zebrafish retina. *J. Theor. Biol.* **200**, 231-244.
- von Dassow, G., Meir, E., Munro, E. M. and Odell, G. M. (2000). The segment polarity network is a robust developmental module. *Nature* **406**, 188-192.
- Waid, D. K. and McLoon, S. C. (1998). Ganglion cells influence the fate of dividing retinal cells in culture. *Development* **125**, 1059-1066.
- Wässle, H., Peichl, L. and Boycott, B. B. (1981a). Morphology and topography of on-alpha and off-alpha cells in the cat retina. *Proc. R. Soc. Lond. B* **212**, 157-175.
- Wässle, H., Boycott, B. B. and Illing, R. B. (1981b). Morphology and mosaic of on-beta and off-beta cells in the cat retina and some functional considerations. *Proc. R. Soc. Lond. B* **212**, 177-195.
- Wässle, H. and Riemann, H. J. (1978). The mosaic of nerve cells in the mammalian retina. *Proc. R. Soc. Lond. B* **200**, 441-461.
- Zhan, X. J. and Troy, J. B. (2000). Modeling cat retinal beta-cell arrays. *Vis. Neurosci.* **17**, 23-39.